British Journal of Pharmacology (2005) 145, 405–414
www.nature.com/bjp

Block of TRPC5 channels by 2-aminoethoxydiphenyl borate: a differential, extracellular and voltage-dependent effect

[1]Shang-Zhong Xu, [1]Fanning Zeng, [2]Guylain Boulay, [3]Christian Grimm, [3]Christian Harteneck & *,[1]David J. Beech

[1]School of Biomedical Sciences, University of Leeds, Leeds LS2 9JT; [2]Department of Pharmacology, Universite de Sherbrooke, Sherbrooke, Quebec, Canada J1H 5N4 and [3]Institut fur Pharmakologie, Charite-Universitatsmedizin Berlin, Campus Benjamin Franklin, Thielallee 69-73, 14195 Berlin, Germany

1 2-Aminoethoxydiphenyl borate (2-APB) has been widely used to examine the roles of inositol 1,4,5-trisphosphate receptors (IP_3Rs) and store-operated Ca^{2+} entry and is an emerging modulator of cationic channels encoded by transient receptor potential (TRP) genes.

2 Using Ca^{2+}-indicator dye and patch-clamp recording we first examined the blocking effect of 2-APB on human TRPC5 channels expressed in HEK-293 cells.

3 The concentration–response curve has an IC_{50} of 20 μM and slope close to 1.0, suggesting one 2-APB molecule binds per channel. The blocking effect is not shared by other Ca^{2+} channel blockers including methoxyverapamil, nifedipine, *N*-propargylnitrendipine, or berberine.

4 In whole-cell and excised membrane patch recordings, 2-APB acts from the extracellular but not intracellular face of the membrane.

5 Block of TRPC5 by 2-APB is less at positive voltages, suggesting that it enters the electric field or acts by modulating channel gating.

6 2-APB also blocks TRPC6 and TRPM3 expressed in HEK-293 cells, but not TRPM2.

7 Block of TRP channels by 2-APB may be relevant to cell proliferation because 2-APB has a greater inhibitory effect on proliferation in cells overexpressing TRPC5.

8 Our data indicate a specific and functionally important binding site on TRPC5 that enables block by 2-APB. The site is only available *via* an extracellular route and the block shows mild voltage-dependence.

British Journal of Pharmacology (2005) **145,** 405–414. doi:10.1038/sj.bjp.0706197
Published online 4 April 2005

Keywords: Cationic channel; calcium channel; transient receptor potential; 2-aminoethoxydiphenyl borate

Abbreviations: 2-APB, 2-aminoethoxydiphenyl borate; BRDU, 5-bromo-2′ deoxy-uridine; CCH, carbachol; CRAC, Ca^{2+}-release activated channel; DAG, diacylglycerol; DMSO, dimethyl sulphoxide; IP_3, inositol 1,4,5-trisphosphate; IP_3R, IP_3 receptor; NMDG, *N*-methyl-D-glucamine; PLC, phospholipase C; SOC, store-operated channel; TG, thapsigargin; TRP, transient receptor potential; TRPC, canonical TRP; TRPM, melastatin TRP

Introduction

The transient receptor potential (TRP) superfamily comprises mammalian genes encoding calcium- and sodium-permeable channels that are divided into six subfamilies: TRPC (canonical), TRPM (melastatin), TRPV (vanilloid), TRPP (polycystin), TRPML (mucolipin) and TRPA (ANKTM1) (Clapham, 2003). The channels have diverse functions including involvement in Ca^{2+} store-operated and G-protein coupled receptor pathways, cell volume regulation, and pheromone, redox, taste and temperature sensation. The TRPC family has seven members, all of which have been associated with Ca^{2+}-permeable ion channel elements of store- and receptor-operated plasma membrane signalling. Based on amino-acid sequence they are subdivided into four groups (TRPC1, TRPC2, TRPC4/5 and TRPC3/6/7). Apart from TRPC2, which is not thought to be expressed in human, TRPC expression may be relevant to a range of human cells in the nervous system, blood vessels and blood cells, gastrointestinal tract and kidney (Sossey-Alaoui *et al*., 1999; Vannier *et al*., 1999; Xu & Beech, 2001; Riccio *et al*., 2002; Zitt *et al*., 2002; Clapham 2003; Beech *et al*., 2004). However, the physiological function and pharmacological regulation of TRPC channels are still unclear.

2-Aminoethoxydiphenyl borate (2-APB) was originally introduced as a membrane-permeable inhibitor of IP_3 receptors (IP_3Rs) and has since been widely used to examine the functions of these receptors and the functions of other Ca^{2+} signalling mechanisms such as store-operated Ca^{2+}-entry (Bootman *et al*., 2002). Commonly, 75 μM 2-APB is sufficient to strongly inhibit Ca^{2+} influx *via* store-operated channels (SOCs) in native cell types (Bootman *et al*., 2002; Ma *et al*., 2002; Flemming *et al*., 2003). Furthermore, micromolar 2-APB has effects on heterologously expressed TRP channels, such as TRPC1 (Delmas *et al*., 2002), TRPC3 (Ma *et al*., 2000; Trebak *et al*., 2002), TRPC5 (Lee *et al*., 2003b), TRPV6 (Voets *et al*.,

*Author for correspondence; E-mail: d.j.beech@leeds.ac.uk
Published online 4 April 2005

2001; Schindl *et al*., 2002), TRPM8 (Hu *et al*., 2004) and TRPV1-3 (Chung *et al*., 2004; Hu *et al*., 2004).

In this study, we explore the mechanism of the effect of 2-APB on human TRPC5 and make comparisons with TRPC6, TRPM2 and TRPM3.

Methods

For studies of human TRPC5 (Accession Number AF054568) and TRPM2 (NM_003307) HEK-293 cells had stable tetracycline (Tet)-regulated expression of cDNA encoding TRPC5 (Zeng *et al*., 2004) or TRPM2 (McHugh *et al*., 2003). Cells were grown in DMEM-F12 (Gibco, U.K.) medium containing 10% fetal calf serum, 100 U ml^{-1} penicillin and 100 μg ml^{-1} streptomycin. Cells were maintained at 37°C under 95% air and 5% CO_2 and replated on coverslips prior to experiments. The expression of TRPC5 and TRPM2 was induced by 1 μg ml^{-1} tetracycline (Tet+) for 24–72 h before recording. Noninduced cells without addition of tetracycline (Tet−) were used as control. HEK-293 cells stably expressing mouse TRPC6 and transiently expressing human TRPM3 have been described (Boulay, 2002; Grimm *et al*., 2003).

Voltage clamp was performed at room temperature (23–26°C) with the whole-cell, inside-out and outside-out patch configurations. Signals were amplified with an Axopatch 200A patch clamp amplifier and controlled with pClamp software 6.0 (Axon). A 1-s ramp voltage protocol from −100 to +100 mV was applied at a frequency of 0.1 Hz and from a holding potential of −60 mV. Signals were digitally sampled at 3 kHz after analogue filtering with a cutoff frequency of 1 kHz. For Figure 5c, data were smoothed by adjacent five-point averaging to reduce noise prior to calculation of the percentage block. For inside-out or outside-out patches and voltage dependence studies, step voltages from −100 to +90 mV were applied and signals sampled at 10 kHz. Patch pipettes were made from borosilicate glass capillary tubing with an outside diameter of 1 mm and inside diameter of 0.58 mm (Clark Electromedical Instruments, Reading, U.K.). After fire-polishing and filling with pipette solution, the resistance of pipettes was 3–5 MΩ. The standard patch pipette solution contained (mM): 135 CsCl, 1 EGTA, 2 $MgCl_2$, 10 HEPES, 5 sodium ATP, 0.1 sodium GTP, pH titrated to 7.2 with CsOH, and osmolarity adjusted to 290 mOsm with mannitol. For some recordings, as indicated, a pipette solution containing 200 nM free Ca^{2+} was used (mM): 115 CsCl, 10 EGTA, 2 $MgCl_2$, 10 HEPES, 5 sodium ATP, 5.7 $CaCl_2$, pH titrated to 7.2 with CsOH, and osmolarity adjusted to 290 mOsm with mannitol. To study the voltage dependence of block, the 200 nM Ca^{2+} pipette solution was used, but with low chloride (120 CsOH, 120 L-glutamic acid, 10 EGTA, 2 $MgCl_2$, 10 HEPES, 5.7 $CaCl_2$, pH 7.2, osmolarity 290 mOsm). For TRPM2 experiments, 0.5 mM ADP-ribose was included in the 200 nM Ca^{2+} pipette solution. The standard bath solution contained (mM): 130 NaCl, 5 KCl, 8 D-glucose, 10 HEPES, 1.2 $MgCl_2$ and 1.5 $CaCl_2$, pH titrated to 7.4 with NaOH. For inside-out patch experiments the bath solution contained (mM): 130 CsCl, 1 EGTA, 2 $MgCl_2$, 10 HEPES, 5 sodium ATP, titrated to pH 7.2 with CsOH; The standard bath solution was in the pipette. The recording chamber had a volume of 150 μl and was perfused at a rate of about 2 ml min^{-1}.

Ca^{2+} imaging was previously described (Xu & Beech, 2001). Cells were preincubated with 1 μM fura PE3-AM at 37°C for 1 h in standard bath solution, followed by a 15–30 min period in standard bath solution at room temperature. The ratio of fura-PE3 fluorescence excited alternately at 340 and 380 nm was monitored (Improvision, U.K.) and emission was collected *via* a 510-nm filter and sampled by a CCD camera (Orca ER; Hamamatsu, Japan). Images were sampled every 10 s in pairs for the two excitation wavelengths and analysed off-line using regions of interest to select individual cells. Imaging was controlled by Openlab 2.0 software (Image Processing & Vision Company Ltd, U.K.). In some cases, store-depletion was achieved by incubating cells for 30 min with 1 μM thapsigargin (TG). TRPM3 methods were as described (Grimm *et al*., 2003). In brief, fluorescence quenching by Mn^{2+} entry was studied using the fura-2 isosbestic excitation wavelength of 360 nm. Measurements were made 200 s after application of 1 mM Mn^{2+} in the presence or absence of 100 μM 2-APB. In all experiments, transfected cells were identified by their YFP-fluorescence at an excitation wavelength of 480 nm. All the experiments were at room temperature.

The 5-bromo-2′ deoxy-uridine (BRDU) labelling kit (Roche) was used for cell proliferation measurement. Tet-induced TRPC5 cells were split onto a 24-well plate and cultured with test substance for 36–72 h and then incubated with BRDU for 2 h. After removal of labelling medium, cells were washed, fixed and incubated with anti-BRDU antibody (1 : 1000) for 2 h at room temperature. Cells were washed three times and added substrate solution for colour development and absorbance measurement.

All salts and reagents were from Sigma (U.K.) or BDH (British Drug House, Poole, U.K.). 2-APB, TG, carbachol (CCH), methoxyverapamil (D600), nifedipine, *N*-propargyl-nitrendipine (MRS 1845), gadolinium chloride (Gd^{3+}) and bovine serum albumin (BSA) were purchased from Sigma. Berberine was from Northeast Pharmaceuticals (China). Fura-PE3 AM was from Molecular Probes. TG (10 mM), fura-PE3 AM (1 mM) and 2-APB (75 mM) were made up as stock solutions (stock concentrations are in parentheses) in 100% dimethyl sulphoxide (DMSO). DMSO (0.1%) had no effect on TRPC5 ionic current ($n=5$; e.g. Figure 1c).

Data are expressed as mean ± s.e.m., where n is the number of individual experiments for electrophysiological recordings and cell proliferation analysis, and the number of cells from at least three independent experiments (one per coverslip) for Ca^{2+} imaging. Data sets were compared using unpaired Student's t-test with significance indicated if $P<0.05$. The concentration of half-maximal inhibition (IC_{50}) of 2-APB was given by curve fitting with the Hill equation.

Results

The Tet-induced expression of human TRPC5 in HEK293 cells was confirmed by Western blotting (Zeng *et al*., 2004). In Ca^{2+}-imaging experiments, CCH acting at endogenous muscarinic receptors evoked a Ca_i^{2+} signal in store-depleted cells only if TRPC5 expression was induced (Tet+, $n=60$–62) (Figure 1a). The effect was enhanced by application of gadolinium (Gd^{3+}, 10 μM) and again there was no effect without TRPC5 (Tet−) (Figure 1a). In whole-cell recordings,

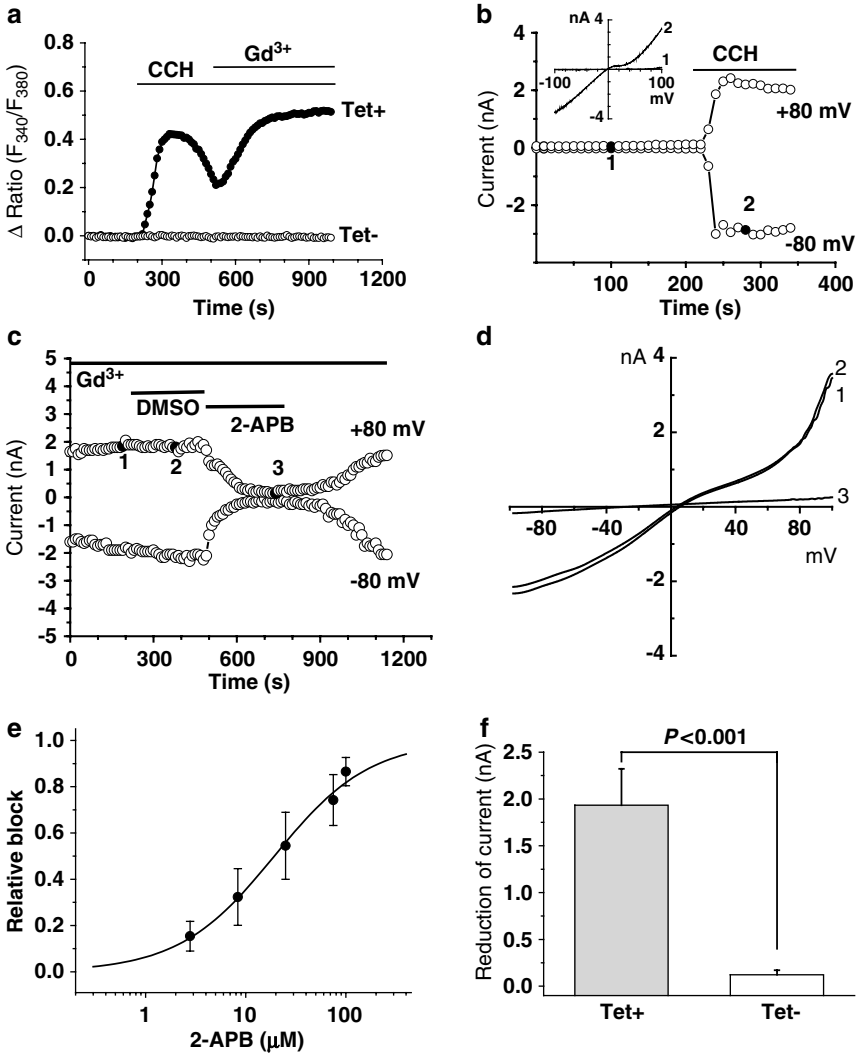

Figure 1 Human TRPC5 signals and concentration-dependent inhibition by 2-APB. (a) Typical Ca^{2+}-imaging data showing carbachol (CCH, 100 μM) induced Ca^{2+} influx in a store-depleted and induced (Tet+, TRPC5-expressing) cell. Gd^{3+} (10 μM) further elevated $[Ca^{2+}]_i$. No Ca^{2+} signal was observed in the noninduced cell (Tet−). (b) Whole-cell voltage-clamp recording showing current sampled every 10 s at +80 and −80 mV from the ramp protocol. The cell was induced (Tet+) and current was activated by CCH (100 μM). Inset: Typical *IV* curves evoked by the ramp voltage protocol before and after activation by CCH. (c) Typical current recording from a Tet+ cell superfused with Gd^{3+} (10 μM). Vehicle control (0.1% DMSO) and then 2-APB (75 μM; DMSO remained at 0.1%) were added to the bath solution for the periods indicated by the horizontal bars. (d) The *IV* curves of TRPC5 for the experiment also shown in (c). (e) Mean±s.e.m. data (filled circles with bars) showing concentration-dependent block of TRPC5 current (at −80 mV) by 2-APB. The fitted Hill equation has a slope of 0.91 and mid-point of 19 μM. (f) Mean±s.e.m. whole-cell current at −80 mV inhibited by 75 μM 2-APB in Tet+ ($n=9$) and Tet− ($n=7$) cells; the two groups are significantly different. The capacitance of the cells was not significantly different: 26.7±4.8 cf 28.5±4.5 pF for Tet+ vs Tet− cells.

CCH activation of TRPC5 was evident as an outward current at +80 mV and inward current at −80 mV ($n=4$) (Figure 1b). The reversal potential was close to 0 mV. CCH had no effect in noninduced cells ($n=4$, data not shown). The current–voltage relationship (*IV*) was similar to that described for mouse TRPC5 (Jung *et al*., 2003), showing inward and outward ('double') rectification, giving something that is roughly 'N-shaped' (Figure 1b, inset). In patch-clamp recordings, a similar current was activated directly by Gd^{3+} (10 μM) in Tet+ cells, whereas there was a small inhibitory effect of Gd^{3+} in noninduced cells (data not shown).

Bath-applied 2-APB essentially abolished TRPC5 current activated by Gd^{3+} (Figure 1c, d), or Gd^{3+} plus CCH (data not shown). The effect occurred promptly and was fully reversible on washout. It was concentration-dependent (IC_{50} 19 μM) and the Hill coefficient was near to 1.0 (Figure 1e). No stimulatory effects were observed (2.8–100 μM 2-APB, $n=6$). In non-induced cells, current was small and had a linear *IV*, unlike that of TRPC5. 2-APB also inhibited this endogenous current but the effect was much smaller than in Tet+ cells (Figure 1f).

TRPC5 can be activated by store-depletion and so may be part of endogenous SOCs, some of which are inhibited by conventional Ca^{2+} channel blockers (Beech *et al*., 2004; Zeng *et al*., 2004). Effects of Ca^{2+} channel blockers on TRPC5 are also possible because there is general structural resemblance of TRP channels to voltage-gated Ca^{2+} channels. Therefore, we considered that established Ca^{2+} channel blockers might affect TRPC5 and possibly mimic the action of 2-APB. Measured by Ca^{2+}-imaging, 10 μM methoxyverapamil (Figure 2a) or 1 μM nifedipine (Figure 2b) had no effect on TRPC5. Berberine

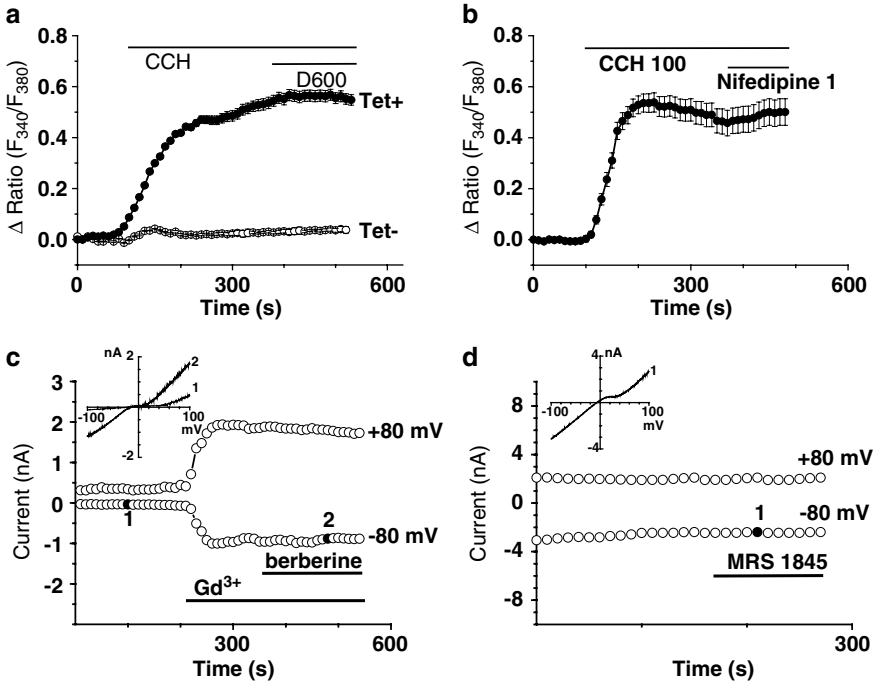

Figure 2 TRPC5 channel is resistant to conventional Ca^{2+} channel blockers. (a) Ca^{2+} imaging data showing no effect of bath-applied methoxyverapamil (D600, 10 μM) in Tet+ or Tet− cells, which were TG-pretreated. (b) No effect of nifedipine (1 μM) on TRPC5 in Tet+, TG-pretreated cells. (c–d) Typical examples of berberine (25 μM) and MRS 1845 (100 μM) on the whole-cell current of TRPC5 activated by Gd^{3+} (10 μM). Insets show the *IV* curves at the corresponding points (filled circles).

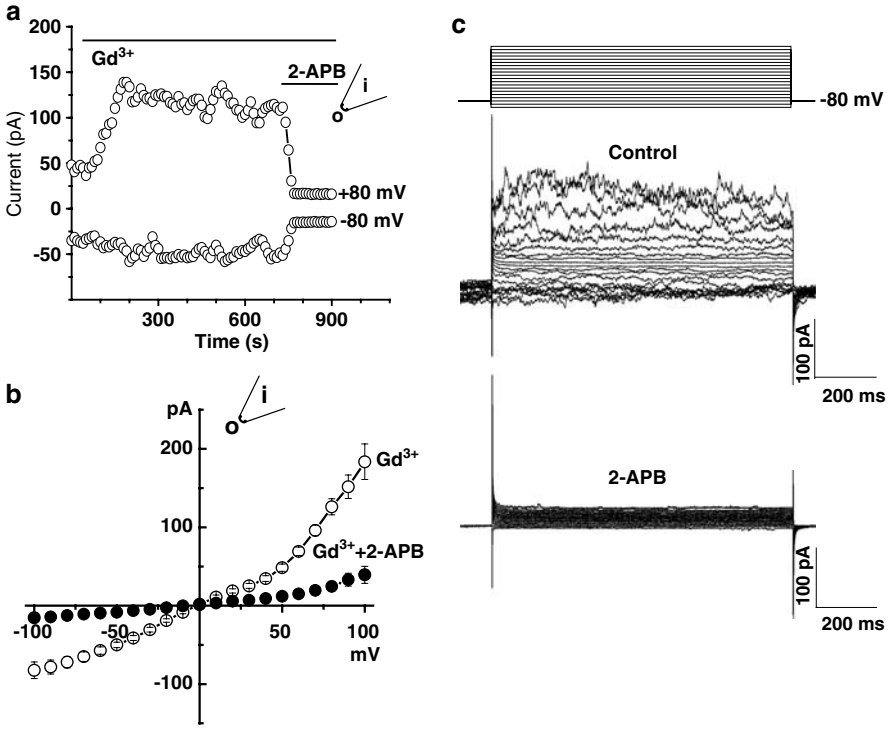

Figure 3 Block of TRPC5 by 2-APB occurs *via* an extracellular site. Recordings were from outside-out patches excised from Tet+ cells. (a) Time-series plot of typical current amplitudes at +80 and −80 mV, showing signals evoked by 10 μM Gd^{3+} and inhibited by 75 μM 2-APB. (b) Mean ± s.e.m. *IV*s in the presence of Gd^{3+} and then Gd^{3+} + 2-APB ($n = 5$ patches). (c) Typical original current traces in response to square voltage steps from −100 to +100 mV. Although this was an excised patch, currents were macroscopic (i.e. discrete unitary current events were not evident) because of the large number of channels expressed.

(25 μM), an L- and a T-type Ca^{2+} current blocker (Xu *et al*., 1997), was tested by whole-cell recording and also had no effect ($n=10$, $P>0.05$; Figure 2c). *N*-propargylnitrendipine (MRS 1845, 10 or 100 μM), a derivative of 1,4-dihydropyridines and blocker of store-operated Ca^{2+} entry in HL-60 cells (Harper *et al*., 2003), had no effect on TRPC5 current ($n=5$, $P>0.05$; Figure 2d). Therefore, there is no functional site for conventional Ca^{2+} channel blockers on TRPC5, and the effect of 2-APB is not related to that of Ca^{2+} channel blockers.

2-APB may suppress function of human TRPC5 either because it inhibits IP_3Rs or because of some other potentially direct effect on the channel. In an effort to explore these possibilities we tested the effect of 2-APB on macroscopic TRPC5-mediated currents in excised membrane patches. In outside-out patch recordings from Tet-induced cells we demonstrated activity of TRPC5 stimulated by Gd^{3+}. This Gd^{3+}-induced current was abolished by bath-applied 2-APB (Figure 3a, b, $n=3$, $P<0.001$). Figure 3c shows typical original current traces for a range of voltages both before (control) and after application of 75 μM 2-APB. The noisy, macroscopic, activity of TRPC5 in the patch was inhibited by 2-APB. A similar blocking effect was observed in outside-out patches if the channel activator was La^{3+} instead of Gd^{3+} (data not shown).

In inside-out patches we demonstrated we had the correct membrane orientation as well as TRPC5 expression by bath-applying the stable GTP analogue GTP-γ-S (20 μM), which induced current (Figure 4a), as in studies of mouse TRPC5 (Jung *et al*., 2003). Bath-application of 2-APB to the intracellular face of the membrane had no effect on TRPC5 (Figure 4c, d). Gd^{3+} also had no stimulating effect when applied intracellularly (data not shown). Concerned that the critical intracellular binding proteins for 2-APB may be lost in excised patches, we also recorded TRPC5 current in whole-cell configuration, applying 2-APB at a high concentration (150 μM) to the inside of the cell *via* the patch pipette. Strikingly, a large TRPC5-mediated current remained 30 min after starting whole-cell recording (Figure 4d, $n=3$). Bath application of 2-APB at half the concentration (75 μM) abolished the TRPC5-mediated current (Figure 4d). Therefore, TRPC5 is resistant to intracellular 2-APB, but blocked by extracellular 2-APB.

Blockade of channels is commonly voltage-dependent, especially when the agent has a charged moiety in its structure, as 2-APB does. To explore if block of TRPC5 by 2-APB has voltage-dependence we preactivated TRPC5 with a lanthanide and applied 2-APB at 20 μM (Figure 5). We also checked the suitability of using a ramp voltage protocol by making comparisons with *IV*s constructed using square steps (Figure 5a, b). The original current traces during square voltage steps show no major time-dependent activation or inactivation events, although a modest decay of current is apparent when the voltage is initially stepped to -80 mV (Figure 5a). Nevertheless, despite this event and the obvious voltage-dependence of TRPC5 (i.e. the *IV* rectifies, Figure 5b), the ramp data align closely with square-step data (Figure 5b), suggesting any voltage-dependent switching events are rapid. Low Cl^- in the pipette solution was used to minimise the risk of contamina-

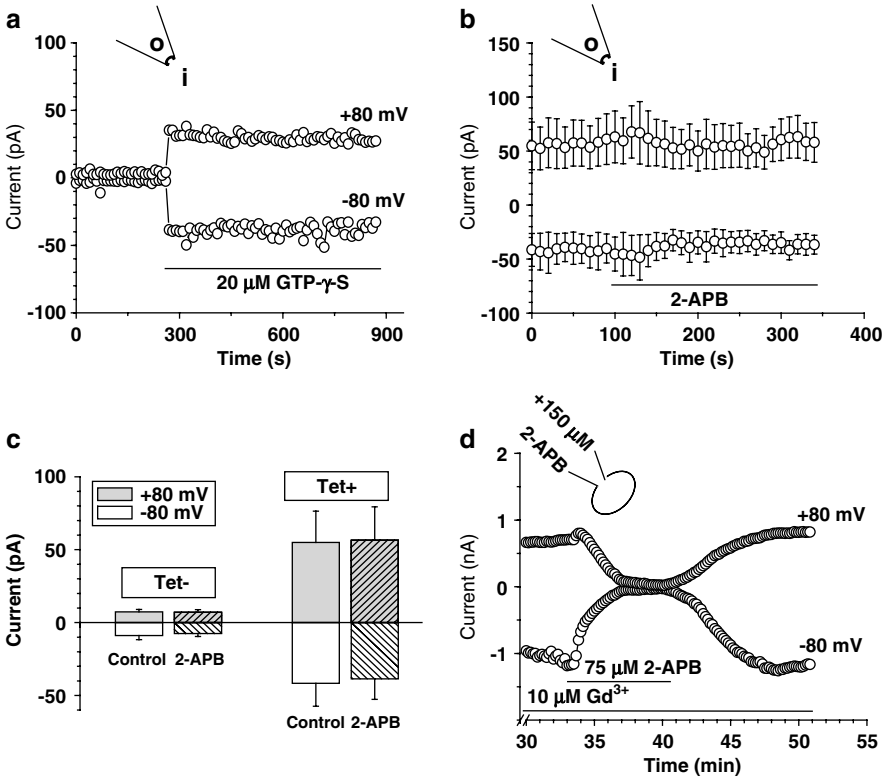

Figure 4 2-APB has no effect when applied to the intracellular face of the membrane. (a) Typical inside-out patch currents at -80 and $+80$ mV recorded from a Tet+ cell and showing TRPC5 current in response to GTP-γ-S. (b) In the presence of 10 μM Gd^{3+} in the pipette (mean$\pm$s.e.m., $n=7$) bath-applied 2-APB (75 μM) had no significant effect. (c) Mean$\pm$s.e.m. inside-out patch currents for Tet+ ($n=7$, $P>0.05$ for control vs 2-APB) and Tet$-$ cells ($n=8$, $P>0.05$ for control vs 2-APB). (d) Typical whole-cell current recorded from a Tet+ cell with 150 μM 2-APB in the patch pipette and 10 μM Gd^{3+} in the bath. The *x*-axis is the time after breaking the cell-attached patch to form the whole-cell. At 33 min, 2-APB (75 μM) was applied to the bath solution.

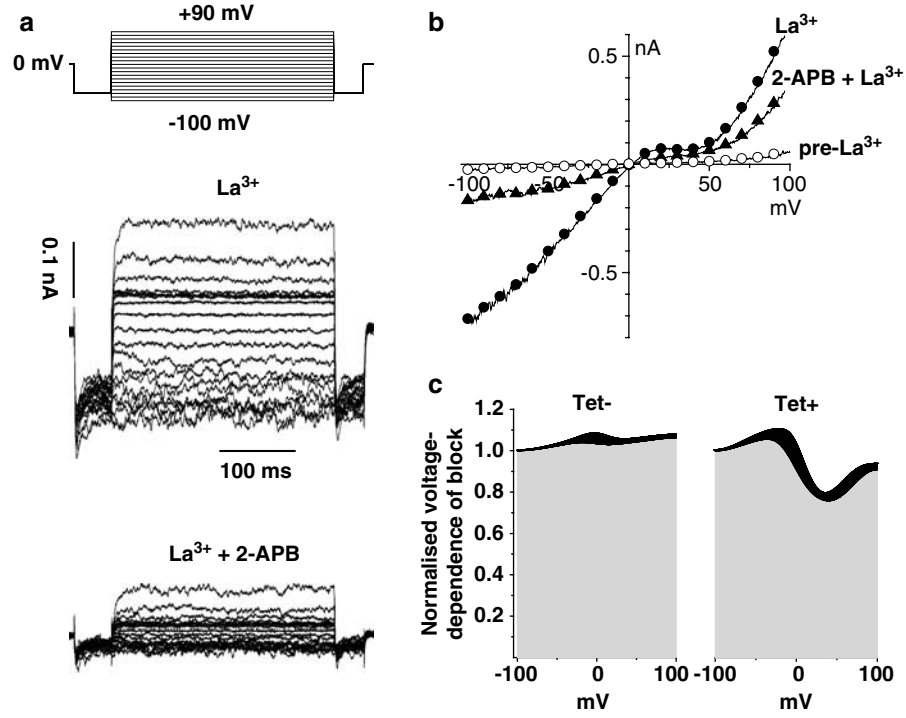

Figure 5 Voltage-dependence of TRPC5 blockade by 2-APB. (a) Currents for a Tet+ cell clamped at membrane potentials from −100 mV to +90 mV by square voltage steps in 10-mV increments. Lanthanum (La^{3+}, 50 μM) was in the bath solution and 2-APB was applied at 20 μM. (b) The symbols show the *IV* curves for the currents before La^{3+}, in La^{3+}, and La^{3+} plus 2-APB, for the data shown in (a). For the same cell, currents in response to the ramp change in voltage are superimposed, showing close alignment with the data from square voltage steps and the suitability of the ramp protocol. The pre-La^{3+} I–V is also shown. (c) The grey shows the mean voltage-dependence of block by 20 μM 2-APB normalised to the percentage block in a given cell at −100 mV. The positive standard errors of the mean are shown in black. Data were obtained using the ramp protocol and are for control cells (Tet−, $n=6$) and cells induced to express TRPC5 (Tet+, $n=5$).

tion from endogenous Cl^- current and neither this (Figure 5b) nor the additional removal of Cl^- from the bath solution by replacement with glutamate (data not shown) changed the 'N' shape *IV* that is characteristic of TRPC5 (cf Figures 1 and 2). The blocking effect of 2-APB on endogenous current in control cells shows little voltage-dependence, contrasting with inhibition of TRPC5 channels, which was weaker at positive membrane potentials (Figure 5c). Similar data were produced using a square-step voltage paradigm (75.8 ± 1.7 and $53.8\pm7.1\%$ block at −80 and +80 mV respectively, $n=5$) or with the ramp protocol and reduced extra- and intracellular Cl^- concentrations (74.2 ± 0.7 and $59.8\pm3.0\%$ block at −80 and +80 mV respectively, $n=3$). Therefore, blockade of TRPC5 by 2-APB has intrinsic voltage-dependence.

Differential effects of inhibitors on related ion channels can help indicate the physical location of the blocking site. Like the action on TRPC5, 2-APB at 75 μM abolished TRPC6 current. The onset of the effect was prompt and the block was readily removed on wash-out (Figure 6a). The reversal potential of TRPC6 current was near 0 mV and the *IV* showed outward rectification (Figure 6b) characteristic of TRPC6 (see review of TRPC6 data in Beech *et al*., 2004). A small effect of 2-APB was observed in control HEK-293 cells (Figure 6c, d), as in Tet− cells (see Figure 1f). The inhibitory effect of 2-APB also occurred in outside-out patch recordings from TRPC6 cells ($n=3$; e.g. Figure 6e, f). TRPM3 is a newly discovered member of the TRP family (Grimm *et al*., 2003; Lee *et al*., 2003a), and was also inhibited by 2-APB: Using an Mn^{2+} quenching protocol (Grimm *et al*., 2003), the tonic Mn^{2+} response in TRPM3-transfected cells was a $39.45\pm9.02\%$ (three independent experiments, $n>20$ cells each) reduction in the F360 signal 200 s after applying Mn^{2+}. In the presence of 2-APB (100 μM) this was significantly reduced to $12.45\pm5.53\%$ ($P<0.05$, three independent experiments), and thus to near the amplitude observed in nontransfected cells ($10.59\pm2.1\%$, four independent experiments). TRPM2 is an important ADP-ribose and Ca^{2+}-activated cationic channel (Perraud *et al*., 2001; McHugh *et al*., 2003). It is characterised by a linear *IV*, a reversal potential close to 0 mV, loss of inward current when Na^+ is substituted by $NMDG^+$, and resistance to Gd^{3+} (Figure 7a, c, d). 2-APB at 75 and 150 μM had no effect on TRPM2-mediated current but the effect on the small background current was evident in Tet− cells (Figure 7b–d).

To address the functional relevance of TRP channel block by 2-APB, we studied cell proliferation. A 36–72 h incubation with 75 μM 2-APB led to strikingly fewer HEK-293 cells compared with control (Figure 8a). This effect might simply be related to inhibition of IP_3R function. However, proliferation of DT40 cells that lack IP_3Rs was also suppressed by 2-APB (Figure 8a), suggesting other mechanisms are involved. To explore this further we determined the effect of 2-APB on BRDU incorporation as a measure of DNA synthesis (and thus cell proliferation) in cells with and without induction of

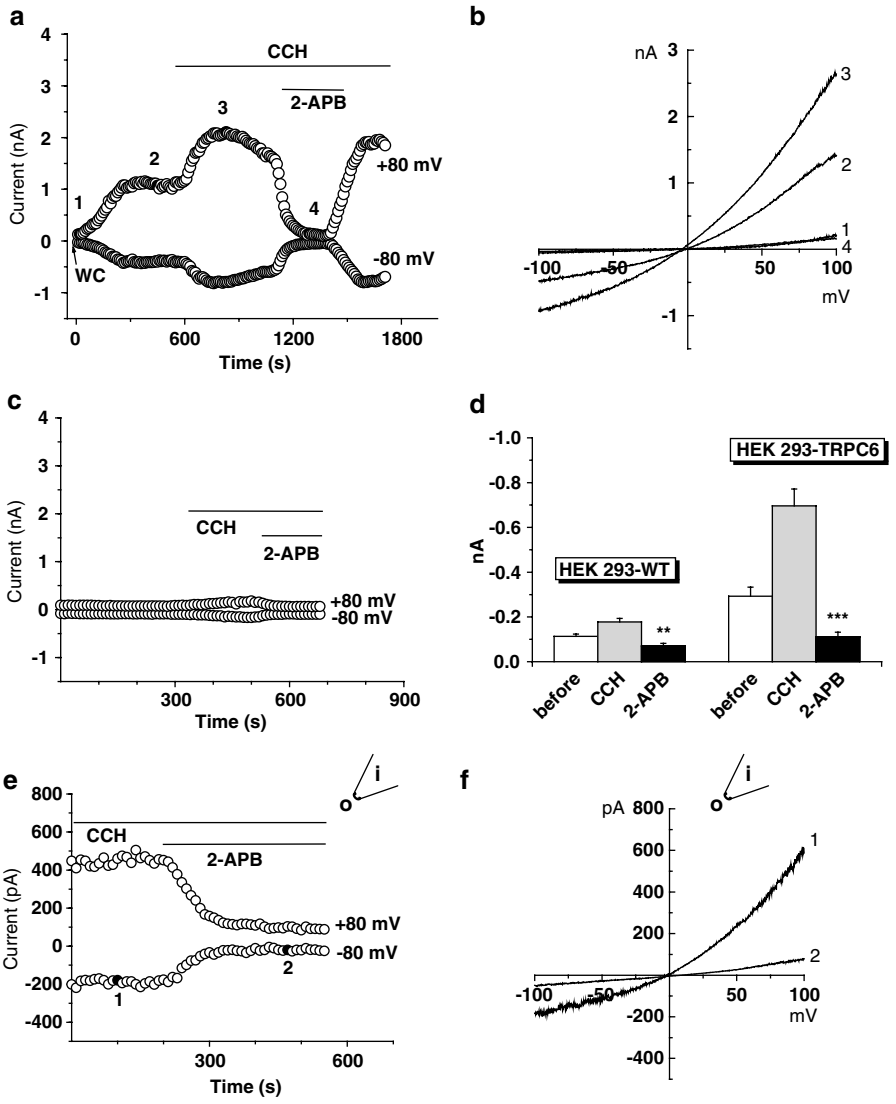

Figure 6 Block of TRPC6 by 2-APB. 2-APB was bath-applied at 75 μM and carbachol (CCH) at 100 μM. (a) For a cell stably expressing TRPC6, current amplitudes recorded using the 200 nM Ca^{2+} pipette solution from the start point of whole-cell recording (WC). (b) *IV* curves from (a). (c) As for (a) but for a wild-type HEK cell. (d) Mean $\pm$ s.e.m. current amplitudes at -80 mV before CCH, after the response to CCH, and after the addition of 2-APB in the presence of CCH. Data are for wild-type cells (WT, $n=5$) and cells stably expressing TRPC6 (TRPC6, $n=7$). $^{**}P<0.01$; $^{***}P<0.001$. (e–f) Recordings from outside-out patches excised from cells stably expressing TRPC6. (e) Time-series plot of typical current amplitudes at $+80$ and -80 mV, showing signals evoked by 100 μM CCH and inhibition by 75 μM 2-APB. (f) *IV*s in the presence of CCH and then CCH + 2-APB (typical of three recordings).

TRPC5 expression. There was significantly greater effect when TRPC5 was expressed (Figure 8b), showing inhibition of cell proliferation by 2-APB is partly related to block of TRP channels.

Discussion

In this study we explored the blockade of TRP channels by 2-APB, focusing particularly on human TRPC5. 2-APB blocks the channel in a concentration-dependent manner and acts exclusively *via* a site that is accessible from the extracellular face of the membrane. This site has specificity for 2-APB because other Ca^{2+} channel blockers are ineffective. The lack of effect of intracellular 2-APB suggests functional IP_3Rs are not required for TRPC5 activation, or blockade by 2-APB. The blockade has an intriguing voltage-dependence, as if 2-APB binds to a membrane-spanning region of the channel within the electric field or modulates TRPC5-gating. Comparison with other TRP channels reveals similar sensitivity of TRPC6 and TRPM3, but resistance of TRPM2. Results from cell proliferation assays indicate 2-APB blockade of TRP channels may be functionally relevant.

Our data are consistent with lanthanides and 2-APB exerting their effects on TRPC5 *via* extracellular sites. The lanthanide effect is comparable to that described for mouse TRPC5, which involves conserved acidic amino acids in the putative outer pore region (Jung *et al*., 2003). 2-APB contains a positively charged group and clearly prevents the functional effect of Gd^{3+}. Such an effect could be explained by competition at a common negatively charged acceptor site.

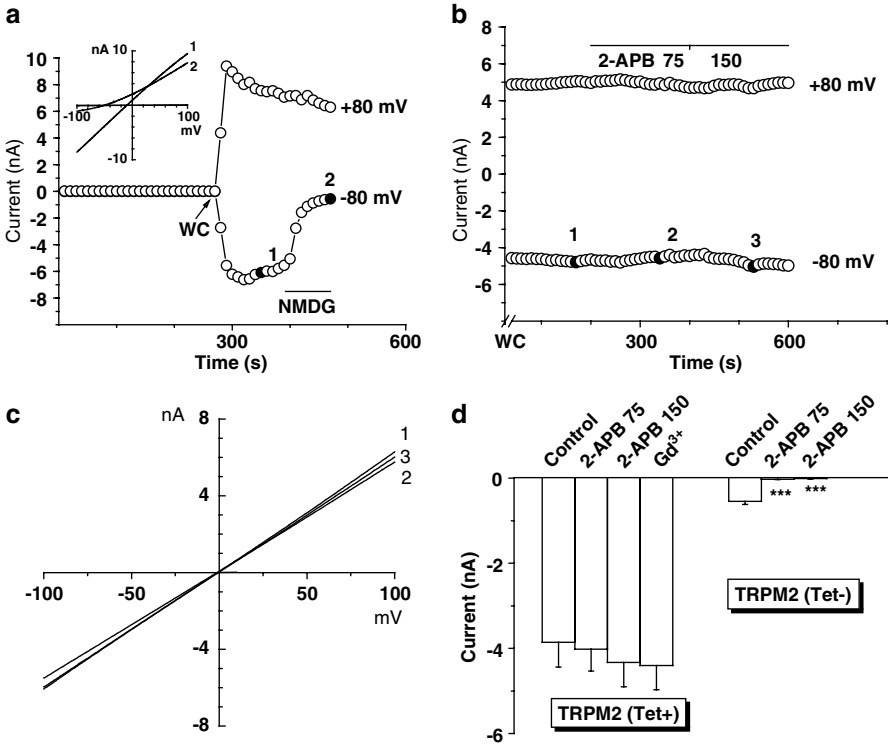

Figure 7 Resistance of TRPM2 to 2-APB. HEK cells were uninduced (Tet−) or induced to express TRPM2 (Tet+). (a) TRPM2 current was induced following break-through to the whole-cell (WC) with the 200 nM Ca^{2+} pipette solution containing ADP-ribose (0.5 mM). Replacement of Na^+ with NMDG inhibited inward current. *IV* curves are inset. Typical of three experiments. (b) Current amplitudes at +80 and −80 mV in a TRPM2 cell and showing the lack of effect of bath-applied 2-APB at 75 and 150 μM. (c) *IV* curves from the experiment shown in (b). (d) Mean ± s.e.m. current amplitudes at −80 mV for TRPM2-expressing (Tet+) cells ($n=7$) and non-induced (Tet−) cells showing endogenous current ($n=3$). ***$P<0.001$.

However, the effects are opposite: lanthanides being stimulatory, 2-APB being inhibitory. Therefore, a more likely explanation is that they act at separate sites, with block of the channel by 2-APB indirectly occluding the activation by lanthanides. Further support for this hypothesis comes from the observation that 2-APB inhibits TRPC6, which does not contain the acidic amino-acid residues involved in stimulation of TRPC5 by lanthanides and is only inhibited by lanthanides.

At the concentrations employed in our study 2-APB is an inhibitor of IP_3Rs and modifies phospholipase C (PLC)γ-induced Ca^{2+} influx in TRPC3-transfected DT40 cells (Bootman *et al*., 2002; Ma *et al*., 2002). Therefore, our observation that there is no intracellular effect of 2-APB indicates IP_3Rs are nonessential for activation of TRPC5. A potential difficulty with using resistance to intracellular 2-APB as evidence for a lack of involvement of IP_3Rs is that block of IP_3Rs by 2-APB depends on the ambient IP_3 concentration – the required 2-APB IC_{50} ranging from 10 μM to 1 mM (Bootman *et al*., 2002). However, this was not a problem in our experiments because IP_3 was not in the whole-cell patch pipette or in the solutions surrounding excised patches and, in most cases, TRPC5 was activated by Gd^{3+} rather than by a G-protein coupled receptor agonist that would stimulate PLC. Therefore, the ambient IP_3 concentration must have been low, making 2-APB potent as an inhibitor of IP_3 Rs. A study of mouse TRPC5 in *Xenopus* oocytes indicated a role for IP_3 and its receptor in TRPC5 activation (Kanki *et al*., 2001). In contrast, studies in HEK-293 and DT40 cells have found no effect of IP_3 and activation in the absence of IP_3R expression (Strubing *et al*., 2001; Venkatachalam *et al*., 2003). Our data on human TRPC5 are consistent with the conclusions of the latter studies.

Voltage-dependent block by an external positively charged substance that enters the ion pore can be explained by electrical repulsion. 2-APB contains positive charge and blocks TRPC5-mediated current and so the voltage-dependence we observe is consistent with 2-APB interacting with the ion pore of TRPC5, and thus amino acids presumably in and around the fifth and sixth membrane spanning regions. The voltage-dependence of the block is nevertheless complex and shows an intriguing inflexion in the same voltage range as the intrinsic *IV* of TRPC5. Therefore, it should not be excluded that 2-APB could, instead, produce voltage-dependent block because it is a gating modifier of TRP channels. Indeed, such an interpretation would more readily pave the way for a unifying hypothesis for 2-APB interaction with TRP channels, explaining why some are blocked, some unaffected and some stimulated. Sensitivity to 2-APB is an emerging common feature of TRP channels. At 10–100 μM, 2-APB is known to block nine of them: TRPC1, TRPC3, TRPC5, TRPC6, TRPV6, TRPM3, TRPM7, TRPM8 and TRPP2 (Ma *et al*., 2000; Voets *et al*., 2001; Delmas *et al*., 2002; Koulen *et al*., 2002; Schindl *et al*., 2002; Trebak *et al*., 2002; Lee *et al*., 2003b; Hanano *et al*., 2004; Hu *et al*., 2004; this study). High micromolar concentrations stimulate three of them: TRPV1, TRPV2 and TRPV3 (Chung *et al*., 2004; Hu *et al*., 2004). TRPC3, TRPV1 and TRPV6 have been observed to be

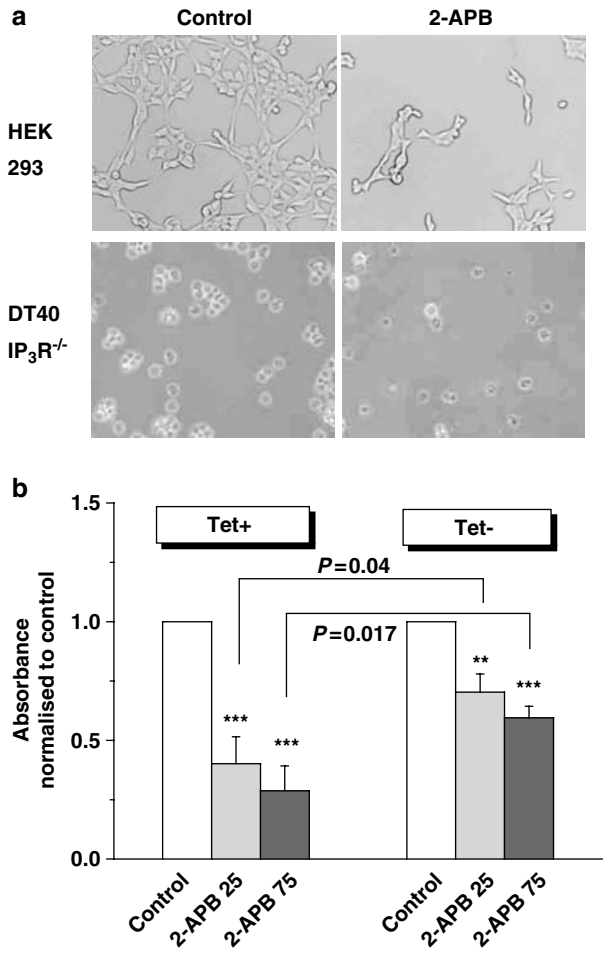

Figure 8 Functional significance of TRP channel block by 2-APB. (a) Phase-contrast images of HEK-293 cells (upper) or triple IP_3R-knockout DT40 cells (lower) after 36–72 h incubation in vehicle (DMSO, Control), or vehicle plus 75 μM 2-APB (2-APB). Images are typical of at least five experiments. (b) *De novo* DNA synthesis indicated by bromodeoxyuridine (BRDU) incorporation detected by absorbance. BRDU incorporation was less after treatment with 2-APB (25 or 75 μM). The effect of 2-APB was significantly greater in Tet+ compared with Tet− cells (four independent experiments for each data point, 11–12 dishes of cells analysed in total). Gd^{3+} (10 μM) and 18-α-glycyrrhetinic acid (50 μM) were present to suppress background channel activity and stimulate TRPC5.

unaffected by 2-APB under some conditions, while TRPV4 and TRPM2 are only known to be resistant (Schindl *et al*., 2002; Trebak *et al*., 2002; Chung *et al*., 2004; Hu *et al*., 2004; this study).

The expression level of TRP family members may affect the activation and pharmacological properties (Voets *et al*., 2001; Schindl *et al*., 2002; Trebak *et al*., 2002). TRPC3 and TRPV6 at low expression level show store-operated properties and both of them are sensitive to 2-APB, but they are resistant to2-APB when highly overexpressed. Regarding the experiments on TRPM2, we cannot exclude the possibility that resistance to 2-APB arises because of a high expression level. However, we find no evidence of such a phenomenon for TRPC5, which was always blocked by 2-APB whether expression levels were low or high, as indicated by ionic current amplitudes over almost two orders of magnitude.

A specific function of TRPC5 in neuronal growth cone formation has been proposed (Greka *et al*., 2003), but otherwise the physiological functions remain to be revealed. Our data now suggest an additional role in cell proliferation. 2-APB also inhibits native SOCs, consistent with the involvement of TRP proteins in this mechanism (Xu & Beech 2001; Flemming *et al*., 2003; Beech *et al*., 2004). The 'CRAC' subtype of SOC is potentiated or inhibited by 2-APB (Prakriya & Lewis, 2001). Like TRP channels, store-operated Ca^{2+}-entry has been associated with cell growth and proliferation (Hunton *et al*., 2002; Sweeney *et al*., 2002).

In conclusion, our data suggest a specific site for 2-APB on TRPC5 channels that is accessible only *via* an extracellular route and most probably involving interaction with the gating mechanism of the channel or a site within the electric field, resulting in an intriguing and previous unrecognised, albeit modest, voltage-dependence to the blockade. We observe differential sensitivity of TRP channels to 2-APB, but sensitivity is nevertheless a common feature, pointing to the existence of a conserved and functionally important drug-binding site on many members of this emerging family of channels.

This work was supported by the Wellcome Trust and British Heart Foundation. We are grateful to AK Srivastava for human TRPC5 DNA fragments, AL Perraud for the TRPM2 cells, and A Tanimura and T Kurosaki for DT40 $IP_3R-/-$ cells.

References

BEECH, D.J., MURAKI, K. & FLEMMING, R. (2004). Non-selective cationic channels of smooth muscle and the mammalian homologues of *Drosophila* TRP. *J. Physiol.,* **559,** 685–706.

BOOTMAN, M.D., COLLINS, T.J., MACKENZIE, L., RODERICK, H.L., BERRIDGE, M.J. & PEPPIATT, C.M. (2002). 2-aminoethoxydiphenyl borate (2-APB) is a reliable blocker of store-operated Ca^{2+} entry but an inconsistent inhibitor of InsP3-induced Ca^{2+} release. *FASEB J.,* **16,** 1145–1150.

BOULAY, G. (2002). Ca^{2+}-calmodulin regulates receptor-operated Ca^{2+} entry activity of TRPC6 in HEK-293 cells. *Cell Calcium,* **32,** 201–207.

CHUNG, M.K., LEE, H., MIZUNO, A., SUZUKI, M. & CATERINA, M.J. (2004). 2-aminoethoxydiphenyl borate activates and sensitizes the heat-gated ion channel TRPV3. *J. Neurosci.,* **24,** 5177–5182.

CLAPHAM, D.E. (2003). TRP channels as cellular sensors. *Nature,* **426,** 517–524.

DELMAS, P., WANAVERBECQ, N., ABOGADIE, F.C., MISTRY, M. & BROWN, D.A. (2002). Signaling microdomains define the specificity of receptor-mediated InsP(3) pathways in neurons. *Neuron,* **34,** 209–220.

FLEMMING, R., XU, S.Z. & BEECH, D.J. (2003). Pharmacological profile of store-operated channels in cerebral arteriolar smooth muscle cells. *Br. J. Pharmacol.,* **139,** 955–965.

GREKA, A., NAVARRO, B., OANCEA, E., DUGGAN, A. & CLAPHAM, D.E. (2003). TRPC5 is a regulator of hippocampal neurite length and growth cone morphology. *Nat. Neurosci.,* **6,** 837–845.

GRIMM, C., KRAFT, R., SAUERBRUCH, S., SCHULTZ, G. & HARTENECK, C. (2003). Molecular and functional characterization of the melastatin-related cation channel TRPM3. *J. Biol. Chem.,* **278,** 21493–21501.

HANANO, T., HARA, Y., SHI, J., MORITA, H., UMEBAYASHI, C., MORI, E., SUMIMOTO, H., ITO, Y., MORI, Y. & INOUE, R. (2004). Involvement of TRPM7 in cell growth as a spontaneously activated Ca^{2+} entry pathway in human retinoblastoma cells. *J. Pharmacol. Sci.,* **95,** 403–419.

HARPER, J.L., CAMERINI-OTERO, C.S., LI, A.H., KIM, S.A., JACOBSON, K.A. & DALY, J.W. (2003). Dihydropyridines as inhibitors of capacitative calcium entry in leukemic HL-60 cells. *Biochem. Pharmacol.,* **65,** 329–338.

HU, H.Z., GU, Q., WANG, C., COLTON, C.K., TANG, J., KINOSHITA-KAWADA, M., LEE, L.Y., WOOD, J.D. & ZHU, M.X. (2004). 2-Aminoethoxydiphenyl borate is a common activator of TRPV1, TRPV2, and TRPV3. *J. Biol. Chem.,* **279,** 35741–35748.

HUNTON, D.L., LUCCHESI, P.A., PANG, Y., CHENG, X., DELL'ITALIA, L.J. & MARCHASE, R.B. (2002). Capacitative calcium entry contributes to nuclear factor of activated T-cells nuclear translocation and hypertrophy in cardiomyocytes. *J. Biol. Chem.,* **277,** 14266–14273.

JUNG, S., MUHLE, A., SCHAEFER, M., STROTMANN, R., SCHULTZ, G. & PLANT, T.D. (2003). Lanthanides potentiate TRPC5 currents by an action at extracellular sites close to the pore mouth. *J. Biol. Chem.,* **278,** 3562–3571.

KANKI, H., KINOSHITA, M., AKAIKE, A., SATOH, M., MORI, Y. & KANEKO, S. (2001). Activation of inositol 1,4,5-trisphosphate receptor is essential for the opening of mouse TRP5 channels. *Mol. Pharmacol.,* **60,** 989–998.

KOULEN, P., CAI, Y., GENG, L., MAEDA, Y., NISHIMURA, S., WITZGALL, R., EHRLICH, B.E. & SOMLO, S. (2002). Polycystin-2 is an intracellular calcium release channel. *Nat. Cell Biol.,* **4,** 191–197.

LEE, N., CHEN, J., SUN, L., WU, S., GRAY, K.R., RICH, A., HUANG, M., LIN, J.H., FEDER, J.N., JANOVITZ, E.B., LEVESQUE, P.C. & BLANAR, M.A. (2003a). Expression and characterization of human transient receptor potential melastatin 3 (hTRPM3). *J. Biol. Chem.,* **278,** 20890–20897.

LEE, Y.M., KIM, B.J., KIM, H.J., YANG, D.K., ZHU, M.H., LEE, K.P., SO, I. & KIM, K.W. (2003b). TRPC5 as a candidate for the nonselective cation channel activated by muscarinic stimulation in murine stomach. *Am. J. Physiol. Gastrointest. Liver Physiol.,* **284,** G604–G616.

MA, H.T., PATTERSON, R.L., VAN ROSSUM, D.B., BIRNBAUMER, L., MIKOSHIBA, K. & GILL, D.L. (2000). Requirement of the inositol trisphosphate receptor for activation of store-operated Ca^{2+} channels. *Science,* **287,** 1647–1651.

MA, H.T., VENKATACHALAM, K., PARYS, J.B. & GILL, D.L. (2002). Modification of store-operated channel coupling and inositol trisphosphate receptor function by 2-aminoethoxydiphenyl borate in DT40 lymphocytes. *J. Biol. Chem.,* **277,** 6915–6922.

MCHUGH, D., FLEMMING, R., XU, S.Z., PERRAUD, A.L. & BEECH, D.J. (2003). Critical intracellular Ca^{2+} dependence of transient receptor potential melastatin 2 (TRPM2) cation channel activation. *J. Biol. Chem.,* **278,** 11002–11006.

PERRAUD, A.L., FLEIG, A., DUNN, C.A., BAGLEY, L.A., LAUNAY, P., SCHMITZ, C., STOKES, A.J., ZHU, Q., BESSMAN, M.J., PENNER, R., KINET, J.P. & SCHARENBERG, A.M. (2001). ADP-ribose gating of the calcium-permeable LTRPC2 channel revealed by Nudix motif homology. *Nature,* **411,** 595–599.

PRAKRIYA, M. & LEWIS, R.S. (2001). Potentiation and inhibition of Ca^{2+} release-activated Ca^{2+} channels by 2-aminoethyldiphenyl borate (2-APB) occurs independently of IP(3) receptors. *J. Physiol.,* **536,** 3–19.

RICCIO, A., MEDHURST, A.D., MATTEI, C., KELSELL, R.E., CALVER, A.R., RANDALL, A.D., BENHAM, C.D. & PANGALOS, M.N. (2002). mRNA distribution analysis of human TRPC family in CNS and peripheral tissues. *Brain. Res. Mol. Brain Res.,* **109,** 95–104.

SCHINDL, R., KAHR, H., GRAZ, I., GROSCHNER, K. & ROMANIN, C. (2002). Store depletion-activated CaT1 currents in rat basophilic leukemia mast cells are inhibited by 2-aminoethoxydiphenyl borate. Evidence for a regulatory component that controls activation of both CaT1 and CRAC (Ca^{2+} release-activated Ca^{2+} channel) channels. *J. Biol. Chem.,* **277,** 26950–26958.

SOSSEY-ALAOUI, K., LYON, J.A., JONES, L., ABIDI, F.E., HARTUNG, A.J., HANE, B., SCHWARTZ, C.E., STEVENSON, R.E. & SRIVASTAVA, A.K. (1999). Molecular cloning and characterization of TRPC5 (HTRP5), the human homologue of a mouse brain receptor-activated capacitative Ca^{2+} entry channel. *Genomics,* **60,** 330–340.

STRUBING, C., KRAPIVINSKY, G., KRAPIVINSKY, L. & CLAPHAM, D.E. (2001). TRPC1 and TRPC5 form a novel cation channel in mammalian brain. *Neuron,* **29,** 645–655.

SWEENEY, M., YU, Y., PLATOSHYN, O., ZHANG, S., MCDANIEL, S.S. & YUAN, J.X. (2002). Inhibition of endogenous TRP1 decreases capacitative Ca^{2+} entry and attenuates pulmonary artery smooth muscle cell proliferation. *Am. J. Physiol. Lung Cell Mol. Physiol.,* **283,** L144–L155.

TREBAK, M., BIRD, G.S., MCKAY, R.R. & PUTNEY JR, J.W. (2002). Comparison of human TRPC3 channels in receptor-activated and store-operated modes. Differential sensitivity to channel blockers suggests fundamental differences in channel composition. *J. Biol. Chem.,* **277,** 21617–21623.

VANNIER, B., PEYTON, M., BOULAY, G., BROWN, D., QIN, N., JIANG, M., ZHU, X. & BIRNBAUMER, L. (1999). Mouse trp2, the homologue of the human trpc2 pseudogene, encodes mTrp2, a store depletion-activated capacitative Ca^{2+} entry channel. *Proc. Natl. Acad. Sci. U.S.A.,* **96,** 2060–2064.

VENKATACHALAM, K., ZHENG, F. & GILL, D.L. (2003). Regulation of canonical transient receptor potential (TRPC) channel function by diacylglycerol and protein kinase C. *J. Biol. Chem.,* **278,** 29031–29040.

VOETS, T., PRENEN, J., FLEIG, A., VENNEKENS, R., WATANABE, H., HOENDEROP, J.G., BINDELS, R.J., DROOGMANS, G., PENNER, R. & NILIUS, B. (2001). CaT1 and the calcium release-activated calcium channel manifest distinct pore properties. *J. Biol. Chem.,* **276,** 47767–47770.

XU, S.Z. & BEECH, D.J. (2001). TrpC1 is a membrane-spanning subunit of store-operated Ca^{2+} channels in native vascular smooth muscle cells. *Circ. Res.,* **88,** 84–87.

XU, S.Z., ZHANG, Y., REN, J.Y. & ZHOU, Z.N. (1997). Effects of berberine of L- and T-type calcium channels in guinea pig ventricular myocytes. *Zhongguo. Yao. Li. Xue. Bao.,* **18,** 515–518.

ZENG, F., XU, S.Z., JACKSON, P.K., MCHUGH, D., KUMAR, B., FOUNTAIN, S.J. & BEECH, D.J. (2004). Human TRPC5 channel activated by a multiplicity of signals in a single cell. *J. Physiol.,* **559,** 739–750.

ZITT, C., HALASZOVICH, C.R. & LUCKHOFF, A. (2002). The TRP family of cation channels: probing and advancing the concepts on receptor-activated calcium entry. *Prog. Neurobiol.,* **66,** 243–264.

(Received December 14, 2004
Revised January 26, 2005
Accepted February 9, 2005)